Organization of Skin Stratum Corneum Extracellular Lamellae: Diffraction Evidence for Asymmetric Distribution of Cholesterol

Thomas J. McIntosh
Department of Cell Biology, Duke University Medical Center, Durham, North Carolina

ABSTRACT   Lipid suspensions containing 2:1:1 skin ceramides:palmitic acid:cholesterol, similar to the lipid composition found in the extracellular matrix of skin stratum corneum, were analyzed by X-ray diffraction methods. These suspensions gave a sharp wide-angle reflection at 4.1 Å, indicating tight hydrocarbon chain packing that would function as a water barrier, and low-angle lamellar diffraction with a repeat period near 130 Å, similar to that previously recorded from intact stratum corneum. The lamellar repeat increased from 121 Å at pH 6 to 133 Å at pH 8.5, allowing phase angles of the lamellar data to be obtained by a sampling theorem "swelling" analysis. Electron density profiles showed that each repeating unit contained two asymmetric bilayers, with a fluid space on one side of the bilayer that increased with increasing pH, due to electrostatic repulsion between bilayers because of ionization of the palmitic acid. Profiles obtained from lamellae with cholesterol sulfate partially substituted for cholesterol showed large density increases on that same side of the bilayer, indicating that cholesterol is asymmetrically distributed in each bilayer. A molecular model was developed postulating that this asymmetry is due to the exclusion of cholesterol from lipid monolayers containing the ester-linked unsaturated (linoleic) hydrocarbon chain of skin ceramide 1. This model can explain the altered organization of extracellular lamellae in epidermal cysts (P. W. Wertz, D. C. Swartzendruber, K. C. Madison, D. T. Downing. 1987. *J. Invest. Dermatol.* 89:419–425) where the ester-linked chains have a higher percentage of saturated fatty acids than found in normal epidermis.

INTRODUCTION

The surface epithelium of mammalian skin, the epidermis, protects the body from desiccation, thus permitting terrestrial mammals to control their internal aqueous balance and survive in a nonaqueous environment (Scheuplein and Blank, 1971; Elias et al., 1977a,b; Forslind, 1994). Moreover, the epidermis protects the body from environmental insults and provides a conduit for absorption of lipid-soluble substances (Scheuplein and Blank, 1971; Elias et al., 1977a,b). Key to this selective permeability barrier is the stratum corneum, the outer epidermal layer, consisting of flattened, anuclate cells surrounded by multiple layers of lipid lamellae (Elias and Friend, 1975; Swartzendruber et al., 1989). In this "brick" (flattened cells) and "mortar" (extracellular lipid) structure, the extracellular lipid forms a continuous domain through the stratum corneum and functions as the major barrier for water diffusion (Elias and Friend, 1975; Elias et al., 1977b). Ineffective epidermal barrier function in several types of pathological states may be due to abnormal extracellular lipid composition, deposition, or organization (Williams and Elias, 1987; Wertz and Downing, 1991; Critchley, 1993).

Both electron microscopy (Elias et al., 1977a,b; Swartzendruber et al., 1989) and X-ray diffraction (White et al., 1988; Bouwstra et al., 1991) demonstrate that the extracellular space in the stratum corneum has a lamellar organization. Freeze-fracture electron microscopy shows that between cells there are multiple lamellar sheets with smooth fracture surfaces (Elias et al., 1977a,b), similar to those observed in lipid multilayers (Costello and Gulik-Krzywicki, 1976). Thin sections also show lamellar arrangement (Elias and Friend, 1975; Elias et al., 1977b; Madison et al., 1987; Swartzendruber et al., 1989), although the appearance of the lamellae depends on the fixation procedure. In particular, the use of ruthenium tetroxide as a secondary fixative gives images of extracellular lamellae with a repeating unit of ~130 Å (Madison et al., 1987; Hou et al., 1991), which is about twice that expected from a single lipid bilayer. In the stratum corneum this repeating unit has alternating electron-dense and electron-lucent bands, with the electron dense bands alternating between "minor dense bands" and "major dense bands" (Madison et al., 1987). That is, each 130 Å repeating unit is centrosymmetric, much like the repeating unit in the nerve myelin sheath. X-ray diffraction patterns of unfixed stratum corneum also give a repeating unit of ~130 Å (White et al., 1988; Garson et al., 1991; Hou et al., 1991; Bouwstra et al., 1994, 1995), along with other wide-angle and low-angle diffraction reflections that have been assigned to lipids or proteins in the stratum corneum. This 130 Å repeating unit has also been obtained from lipid suspensions containing appropriate mixtures of the major lipid components of the stratum corneum—i.e., skin ceramides, free fatty acids, and cholesterol (McIntosh et al., 1996). Interestingly, the 130 Å repeating unit depends on the presence of specific ceramides found in the skin, as well as free fatty acids and cholesterol (McIntosh et al., 1996; Bouwstra et al., 1999, 2001).

Although the lamellar nature of the extracellular region of the stratum corneum has been clearly demonstrated, the organization of these lamellae has been the object of study and speculation for many years. In particular, there have

---

been several models for the structure of the 130 Å repeating unit characteristic of the stratum corneum (White et al., 1988; Swartzendruber et al., 1989; Bouwstra et al., 1991, 1994). For example, White et al. (1988), assuming that the unit cell of the extracellular domain has a bilayer-type configuration and noting that the 130 Å repeat period is much larger than that of a single bilayer, raised the possibilities that the 130 Å repeating unit consisted of "two apposed asymmetric bilayers, symmetric bilayers with asymmetrically distributed protein, or a combination of the two." However, the observation of this 130 Å repeating unit in pure lipid mixtures (McIntosh et al., 1996) appears to eliminate the possibility of asymmetrically distributed protein as the source of this structure, and demonstrates that the lipid components alone must be involved. Based solely on the lipid components, several quite different models for the 130 Å repeating unit have been proposed, including models containing two bilayers (Bouwstra et al., 1994), three bilayers (Bouwstra et al., 1994), and a structure with three hydrocarbon regions, including two bilayers and an intermediate structure with the dimensions of half a bilayer (Swartzendruber et al., 1989; Bouwstra et al., 1991).

This article pursues the question of the organization of this fundamental 130 Å repeating unit by determining the phase angles of the lamellar diffraction reflections and calculating low-resolution electron density profiles for a lipid suspension approximating the lipid composition found in the extracellular matrix of the stratum corneum (Abraham and Downing, 1992; Downing, 1992; McIntosh et al., 1996). The lipid suspension studied is a 2:1:1 mol ratio of skin ceramides:cholesterol:palmitic acid, with the skin ceramides given in Fig. 1. In addition, experiments are performed testing the hypothesis that this 130 Å repeating unit is caused by an asymmetric distribution of cholesterol due to the packing
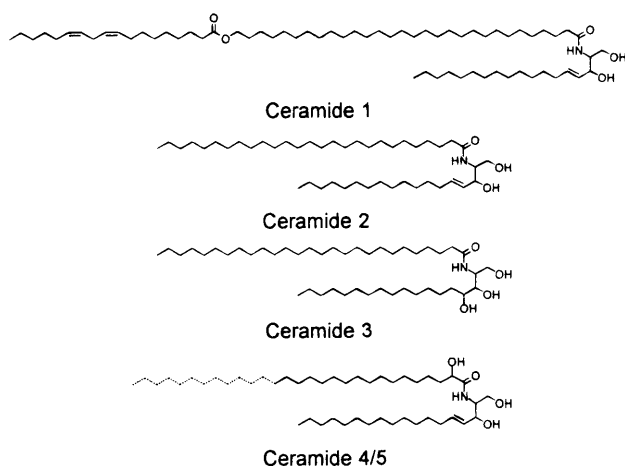

FIGURE 1 Molecular structures of the major porcine skin ceramides. Ceramides 4 and 5 differ only in the chain-length of the α-hydroxy acid moiety (longer in ceramide 4). (Reproduced with permission from McIntosh et al., 1996, copyright American Chemical Society.)

properties of particular skin ceramides. This is accomplished by determining electron density profiles for lipid mixtures where electron rich cholesterol sulfate has been partially substituted for cholesterol.

MATERIALS AND METHODS

Cholesterol, cholesterol sulfate, palmitic acid, HEPES (n-(2-hydroxy-ethyl)-piperazine-n'-2-ethanesulfonic acid), MES (2-[n-Morpholino]ethanesulfonic acid), and Tris buffer were obtained from Sigma Chemical Company (St. Louis, MO). Skin ceramides (Fig. 1) were the kind gift of Drs. Donald T. Downing and Mary Ellen Stewart of the Department of Dermatology at the University of Iowa. These skin ceramides were isolated from pig epidermis by the methods detailed in McIntosh et al. (1996). In brief, the epidermis was heat-separated by the procedures of Hedberg et al. (1988) and the lipid was extracted from the epidermal sheets with 2:1 v:v chloroform:methanol. Aliquots containing ~35 mg of lipid were applied as streaks to 20 × 20-cm thin-layer chromatography plates coated with a 25-mm-thick layer of silica gel (soft layer Adsorbosil plates, Alltech Associates, Deerfield, IL). The chromatograms were developed to the top first in chloroform-methanol-acetic acid, 190:9:1 (v:v:v), and then in ether-acetic acid, 99:1 (v:v). Under these conditions, proteins do not move from the origin of the thin-layer chromatography plate. Bands were located by spraying the chromatograms with a 0.2% solution of dichlorofluorescein in ethanol, allowing the plates to dry, and then viewing them under UV light. The silica gel from the areas of the chromatograms containing the ceramides was scraped off the plates and eluted with 2:1 chloroform:methanol. To remove the dichlorofluorescein, the lipids were applied to small columns of magnesium hydroxide in Pasteur pipettes and the lipid was eluted with 2:1 chloroform:methanol.

Lipid specimens for X-ray diffraction analysis were prepared by the following procedures. The appropriate mixtures of skin ceramides, palmitic acid, cholesterol, or cholesterol sulfate were codissolved in chloroform:methanol (2:1 v:v). After the solvent was removed by rotary evaporation, the lipid mixtures were hydrated in excess buffer by heating the suspensions three times to 80°C for 30 min. To change the ionization state of the palmitic acid, three buffers were used: 20 mM MES, 100 mM NaCl at pH 6.0; 20 mM HEPES, 100 mM NaCl at pH 7.0; or 20 mM Tris, 100 mM NaCl at pH 8.5. The hydrated lipids were sealed in thin-walled X-ray capillary tubes and studied with two different X-ray camera systems. Wide-angle patterns (spacings from 50 to 3 Å, including reflections near 4 Å arising from the lipid hydrocarbon chains) were recorded with a point-collimation camera and low-angle patterns (spacings from 150 Å to 15 Å) were recorded using a mirror-mirror camera (McIntosh and Simon, 1986b; McIntosh et al., 1992b, 1996). All diffraction patterns were recorded at ambient temperature (20°C) on Kodak DEF-5 film loaded in flat plate cassettes.

To obtain electron density profiles across the bilayer, a Fourier analysis of the low-angle X-ray diffraction patterns was performed. Integrated intensities were obtained for each diffraction order by taking densitometer traces along radial lines, measuring the area under each diffraction peak for each trace, and averaging the peak intensities from the traces. Structure amplitudes were calculated from these integrated intensities by applying standard correction factors for unoriented specimens (McIntosh and Simon, 1986a,b) and normalizing by the procedures of Blaurock (1971). The structure amplitude at the origin, $F(0)$, was estimated by assuming that all first-order reflections had the same phase and extending a smooth curve through these orders to the origin of reciprocal space. (Only a rough estimate of $F(0)$ was necessary for the sampling theorem analysis described below, and $F(0)$ was not used in the calculation of electron density profiles.) As described in detail previously (McIntosh and Simon, 1986b; McIntosh and Holloway, 1987; McIntosh et al., 1992a), phase angles were determined by using the lamellar diffraction data with different repeat periods to trace out the continuous transform of the bilayer. For each bilayer system, continuous transforms were calculated by use of the sampling theorem (Shannon, 1949; Worthington et al., 1973) for one data set for each possible phase

combination. The phase combination that gave the best match to the other structure factors was selected (McIntosh et al., 1984; McIntosh and Holloway, 1987). Electron density profiles across the bilayer were calculated from Fourier reconstructions using the X-ray structure factors

$$\rho(x) = (2/d)\Sigma \exp\{i\phi(h)\} \times F(h) \times \cos(2\pi xh/d), \quad (1)$$

where $F(h)$ is the X-ray structure amplitude of order h, x is the distance from the center of the unit cell, d is the repeat period, $\phi(h)$ is the phase angle of order h, and the sum is from $h = 1$ to 3. For centrosymmetric systems (systems where there is a center of symmetry in the middle of the unit cell), each phase angle is either 0 or 180°. The micrographs of Madison et al. (1987) provide excellent evidence that the 130 Å repeating unit is indeed centrosymmetric.

RESULTS

Three diffraction patterns from separate 2:1:1 skin ceramide:palmitic acid:cholesterol suspensions at pH 7.0 each contained a sharp wide-angle reflection at 4.1 Å and three orders of a lamellar repeat period that ranged between 126 and 128 Å. These patterns were similar to those previously observed with similar conditions (McIntosh et al., 1996). A typical low-angle diffraction pattern is presented in Fig. 2, showing the three lamellar reflections. Diffraction patterns recorded at pH 6 and pH 8.5 all gave the same sharp wide-angle reflection at 4.1 Å. However, the lamellar repeat period and the intensity distribution of the low-angle reflections depended on pH. The repeat period at pH 6.0 was 121 Å, whereas the repeat periods for two experiments at pH 8.5 were 132 and 133 Å.

Structure amplitudes for these diffraction patterns from 2:1:1 skin ceramide:palmitic acid:cholesterol are shown as solid circles in Fig. 3. With the assumption that the unit cell (of 121 Å to 133 Å) is centrosymmetric, each diffraction order must have a phase angle of 0 or 180°, or a sign of + or −. Thus, there are $2^3 = 8$ possible phase (sign) combinations for the three diffraction orders. The continuous Fourier transforms can be calculated by use of the sampling theorem (Shannon, 1949) for any one set of data with the correct phase
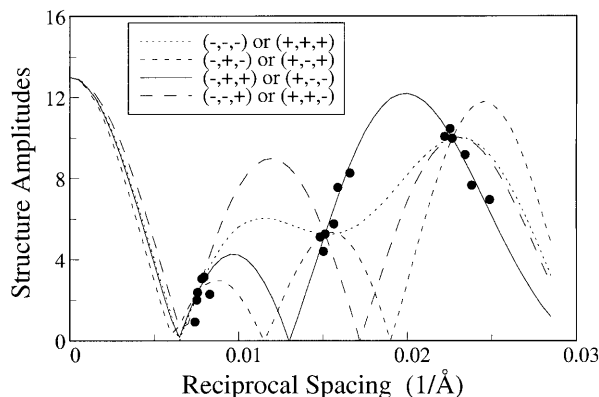
FIGURE 3 Structure amplitudes plotted versus reciprocal spacing for six different suspensions of 2:1:1 skin ceramide:palmitic acid:cholesterol, with repeat periods ranging from $d = 121$ Å to $d = 133$ Å. The solid, dotted, small dashed, and large dashed lines are absolute values of continuous transforms for one particular data set ($d = 132$ Å) with the phase combinations indicated in the figure.

combination, with the ambiguity that the exact opposite phase combination gives continuous transforms with the same absolute values. Fig. 3 shows the absolute values of continuous transforms corresponding to the eight phase choices for one set of data ($d = 132$ Å). All of these transforms are constrained to pass through the structure amplitudes corresponding to $d = 132$ Å, the three circles in Fig. 3 where the four curves cross. However, only the correct phase combination would be expected to match the structure amplitudes for the other data sets. It can be seen from Fig. 3 that the structure amplitudes for all of the data fall closely only to the continuous transform calculated for the combination $(-,+,+)$ or $(+,-,-)$, indicating that one of these combinations is the correct phase choice. However, electron density profiles for swelling experiments with 2:1:1 skin ceramide:palmitic acid:cholesterol and for 2:1:0.5:0.5 skin ceramide:palmitic acid:cholesterol:cholesterol sulfate (see below) are consistent only with the $(-,+,+)$ combination.

Fig. 4 shows the structure factors, structure amplitudes with the correct sign combination of $(-,+,+)$, for the 2:1:1 skin ceramide:palmitic acid:cholesterol experiments and for a 2:1:0.5:0.5 skin ceramide:palmitic acid:cholesterol sulfate preparation at pH 7. Although all of the structure factors for 2:1:1 skin ceramide:palmitic acid:cholesterol fell quite closely to the continuous transform, the structure amplitudes for the 2:1:0.5:0.5 skin ceramide:palmitic acid: cholesterol:cholesterol sulfate fell off the continuous transform. This indicates, as expected, that replacing some of the cholesterol with cholesterol sulfate, with its relatively high electron density sulfate moiety, modified the electron density distribution in the lamellae. It should be noted that specimens composed of 2:1:1 skin ceramide:palmitic acid:cholesterol sulfate (that is, complete substitution of cholesterol sulfate for cholesterol) gave extra reflections at 41 Å, indicating phase separation.
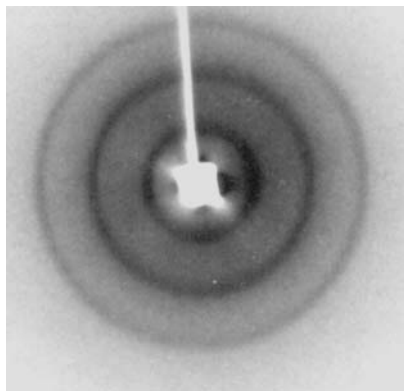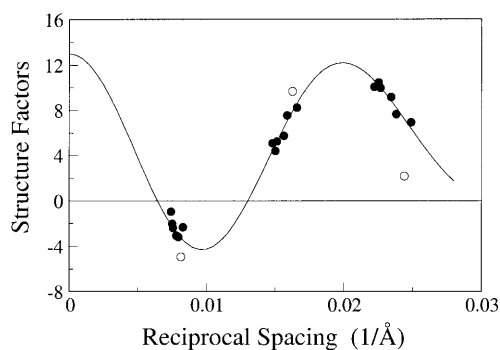

FIGURE 2 Low-angle X-ray diffraction pattern for a suspension of 2:1:1 skin ceramides:palmitic acid:cholesterol in buffer at pH 7. Three diffraction rings are visible—the first three orders of a 126-Å lamellar repeat period.

FIGURE 4 Structure factors for 2:1:1 skin ceramide:palmitic acid:cholesterol (*solid circles*) and 2:1:0.5:0.5 skin ceramide:palmitic acid:cholesterol:cholesterol sulfate (*open circles*). The solid line is the continuous Fourier transform for 2:1:1 skin ceramide:palmitic acid:cholesterol calculated using the sampling theorem for the $d = 132$ Å data set.

Fig. 5 shows electron density profiles calculated using the phases $(-,+,+)$ for 2:1:1 skin ceramide:palmitic acid: cholesterol for the observed minimum ($d = 121$ Å) and maximum ($d = 133$ Å) repeat periods. These low-resolution ($d/2h_{max} = 20$ to 22 Å) profiles contained three high electron density peaks, centered at 0 Å and $+/- 47$ Å, and two low-density dips at $+/- 22$ Å. In this figure, the $d = 133$ Å profile was slightly shifted vertically so that the low density dips in the two profiles had the same relative electron density. The positions and widths of these three peaks and two dips were nearly the same for these minimum and maximum different repeat periods (Fig. 5), as well as for intermediate repeat periods (profiles not shown). These profiles are consistent with the unit cell containing two asymmetric bilayers, with the low density hydrocarbon regions of the two bilayers centered at $+/- 22$ Å and the headgroups of one bilayer located at 0 Å and 47 Å and the headgroups of the apposing bilayer located at $- 47$ Å and 0 Å. (Note that although each bilayer is asymmetric, the unit cell is centrosymmetric with a center of symmetry at 0 Å between adjacent bilayers.) At this resolution the space between adjacent bilayers at 0 Å was not resolved, whereas small gaps between adjacent bilayers were present at the outer edges of the profiles. Moreover, at the outer edges of the profiles the medium density region was
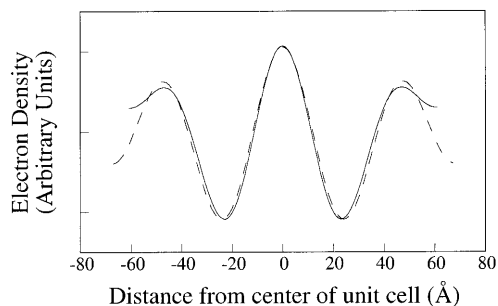
wider and had a lower electron density for the $d = 133$ Å (pH 8.5) profile than for the $d = 121$ Å (pH 6.0) profile. This is consistent with the lamellae taking up more water at pH 8.5 than at pH 6.0, and thus having a wider fluid space between unit cells. The presence of these variable-width intermediate density fluid regions at the outer edges of the profile proves that the phase choice $(-,+,+)$ is correct, rather than $(+,-,-)$, as the electron density of buffer is higher than that of hydrocarbon, but lower than that of the lipid headgroups (Franks, 1976; McIntosh and Simon, 1986b).

Fig. 6 shows profiles of 2:1:1 skin ceramide:palmitic acid:cholesterol and 2:1:0.5:0.5 skin ceramide:palmitic acid:cholesterol:cholesterol sulfate. In this figure, the ceramide:palmitic acid:cholesterol:cholesterol sulfate profile was shifted vertically so that the low-density dips (at $+/- 22$ Å) in the two profiles had the same relative electron density. With this slight shift, the profiles were similar from -40 Å to $+ 40$ Å. However, the electron density at the outer edge of the headgroup peaks at $+/- 47$ Å was much higher in the cholesterol sulfate-containing system. Note that if the exact opposite phase combination $(+,-,-)$ were used, the profiles would be upside-down and the addition of cholesterol sulfate would decrease the electron density—clearly, not a physically reasonable alternative. Thus, the profiles of Fig. 6 indicate that cholesterol sulfate was preferentially located in one headgroup of each bilayer in the unit cell.

DISCUSSION

The electron density profiles obtained in this article provide new information on the organization of the large (~ 130 Å) repeating unit that is a characteristic feature of the functionally important extracellular matrix in the skin stratum corneum. Although the ~ 130 Å repeat period has been observed for several years from both intact stratum corneum (White et al., 1988; Bouwstra et al., 1994) and isolated skin lipids (McIntosh et al., 1996; Bouwstra et al., 1996), electron density profiles have not previously been calculated because the phases of the reflections had not been obtained.

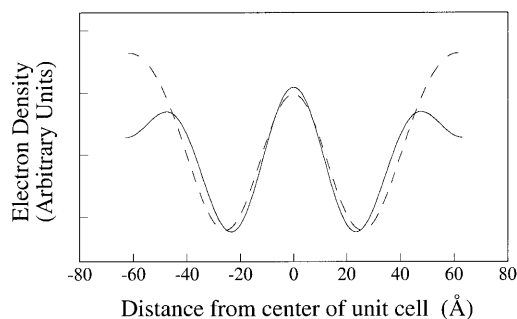This article uses the "swelling" method to trace out the

FIGURE 5 Electron density profiles for 2:1:1 skin ceramide:palmitic acid:cholesterol suspensions at pH 6.0 (*solid line*) and pH 8.5 (*dotted line*).

FIGURE 6 Electron density profiles for 2:1:1 skin ceramide:palmitic acid:cholesterol (*solid line*) and 2:1:0.5:0.5 skin ceramide:palmitic acid: cholesterol:cholesterol sulfate (*dotted line*).

continuous Fourier transform of the lipid structure (Levine and Wilkins, 1971; Worthington et al., 1973; Franks, 1976; Torbet and Wilkins, 1976; McIntosh and Simon, 1986b). Previously this swelling method could not be used with the diffraction from stratum corneum or skin lipids because the repeat period was insensitive to water content (Bouwstra et al., 1994; McIntosh et al., 1996). However, in this article a limited amount of "swelling" (from $d = 121$ Å to $d = 133$ Å) was obtained by changing the pH from 6 to 8.5. This increase in pH would be expected to charge palmitic acid, the only ionizable lipid in this pH range in the skin ceramide:cholesterol:palmitic acid system. It should be noted that the repeat period of nerve myelin also increases with increasing pH due to the surface charge on the myelin membrane (Inouye and Kirschner, 1988). Although there was only a modest change in repeat period with the skin lipids, it allowed observation of enough points on the continuous transform so that sampling theorem analysis showed that only one set of phases (and its exact opposite) was consistent with all the diffraction data from all swelling experiments (Fig. 3). The one ambiguity in phase combination was eliminated by consideration of profiles at different degrees of swelling (Fig. 5) and with cholesterol sulfate (Fig. 6).

The profiles of Fig. 5 show several organizational features of the large (~130 Å) repeat period. First, the profiles (resolution $d/2h_{max} = 20-22$ Å) clearly show that the unit cell contains only two bilayers, with the low density troughs located +/− 22 Å representing the centers of the hydrocarbon regions and the peaks at 0 Å and +/− 47 Å representing the headgroup peaks. The profiles of each bilayer in Fig. 5 are similar in shape to the bilayer profiles obtained from nerve myelin membranes at similar resolution ($d/2h_{max} = 17$ Å) (McIntosh and Worthington, 1974). Second, the profiles show that there is an asymmetry in each bilayer, with the headgroup peaks on the outer edge of each profile (+/− 47 Å) being of lower density than the merged headgroup peaks at 0 Å. In addition, the profiles show that the increased repeat period due to raising the pH was due to an increase in distance between each pair of bilayers. That is, as the pH was increased the medium density (water) layer at the outside edges of the profiles increased in width, with no comparable increase in distance between the bilayers at the center of profile (0 Å).

Although the profiles in Fig. 5 are at high enough resolution to prove that there are only two bilayers per 130 Å unit cell, the profiles by themselves are not at sufficient resolution to provide additional details on the molecular organization of each bilayer. However, the profiles of Fig. 6 show that the partial substitution of cholesterol with cholesterol sulfate increases the electron density in the headgroup regions primarily on one side of the bilayer, the same side of the bilayer where the pH-induced increase in repeat period occurred. Since both the lamellar repeat period and wide-angle spacing are very similar for 2:1:1 skin ceramide:palmitic acid:cholesterol and 2:1:0.5:0.5 skin

ceramide:palmitic acid:cholesterol:cholesterol sulfate samples, it appears that cholesterol sulfate does not change the molecular organization of the lamellae. Thus the profiles of Fig. 6 provide strong evidence that the asymmetry in each bilayer is due, at least in part, to an asymmetrical distribution of cholesterol, and that an appreciable concentration of palmitic acid must also be located on the same side of the bilayer as the high concentration of cholesterol.

There are two possible reasons that the pairs of bilayers in the 130 Å unit cell swell apart, and yet there is no observable swelling in the center of the unit cell with increasing pH (Fig. 5). One possibility, mentioned above, is that the palmitic acid is preferentially localized in the outer monolayer of each bilayer in the profile. A second possibility, suggested previously by Swartzendruber et al. (1989), is that some of the ceramides might insert one of their hydrocarbon chains into one bilayer and the other hydrocarbon chain into the apposing bilayer. That is, the two hydrocarbon chains of the ceramide molecule would face in opposite directions, rather than the tuning-fork arrangement shown in Fig. 1. Such a chain-sharing arrangement could hold the apposing bilayers together at the center of each profile, and be a reason for the fact that headgroup peaks from apposing bilayers are not resolved at 0 Å (Fig. 5). These profiles are not at high enough resolution to distinguish between these two possibilities.

The profiles in Fig. 5 are consistent with transmission electron microscopic (TEM) images of the lipid lamellae in the stratum corneum (Madison et al., 1987; Hou et al., 1991). That is, both the electron density profiles and the TEM images show uniform thickness hydrocarbon regions with variations in the density and thickness of alternating bilayer headgroup regions. In both X-ray diffraction and TEM images of the stratum corneum the width of the unit cell is ~130 Å.

Based on this X-ray analysis and previous structural investigations, the following model for the molecular organization and formation of the 130 Å repeating unit of the skin stratum corneum is proposed. In this model, each bilayer contains a more or less symmetric arrangement of most skin ceramides (ceramides 2–5), but an asymmetric arrangement of ceramide 1 and cholesterol. The profiles of Fig. 6 demonstrate the asymmetrical arrangement of cholesterol, and the following arguments support a complementary asymmetric arrangement of ceramide 1, which constitutes ~10% of the total ceramide in the stratum corneum (Downing, 1992). It has been shown in phospholipid systems that cholesterol preferentially interacts with saturated hydrocarbon chains compared to unsaturated chains (Needham and Nunn, 1990; Smaby et al., 1997; Brzustowicz et al., 2002). Most of the free fatty acids and ceramide hydrocarbon chains in the stratum corneum are saturated (Wertz and Downing, 1991), with one exception being the doubly unsaturated ester-linked linoleic chain of ceramide 1 (Fig. 1). Thus, we argue that cholesterol's preference for saturated chains over unsaturated chains could

drive the formation of the asymmetrical bilayer. That is, cholesterol would prefer to be in the monolayer of the bilayer with free fatty acid and a fraction of ceramides 2–5, but avoid interaction with the linoleic chain of ceramide 1 which would be preferentially located in the apposing monolayer of the bilayer. (The relatively large electron density in the center of the unit cell in the profiles of Fig. 5 is also consistent with such an asymmetric location of ceramide 1. That is, if the two oxygens of the ester linkage of the linoleic chain were located in this headgroup region they could slightly increase its electron density.) Ceramide 1 appears to be critical for the formation of the 130 Å repeat period (McIntosh et al., 1996; Bouwstra et al., 2002). Moreover, Bouwstra et al. (2002), using synthetic analogs of ceramide 1, have recently shown the importance of the linoleic chain. That is, when the linoleic chain was replaced with a saturated (stearate) hydrocarbon chain, the 130 Å structure was not observed and a 63 Å periodicity was observed instead (Bouwstra et al., 2002).

The importance of the linoleic chain in the formation of the 130 Å repeating unit might help explain some unusual properties of epidermal cysts. In these cysts there is an abnormally low content of the ester-linked linoleic chain in ceramide 1 (Wertz et al., 1987). As described above, this could prevent the formation of the 130 Å structure found in the extracellular lamellae of normal stratum corneum with its characteristic TEM appearance of alternating light and dark dense bands (Madison et al., 1987). Indeed, in the extracellular lamellae in epidermal cysts there is no such asymmetric structure, so that in TEM images, the dark bands across the lamellar array are of uniform density (Wertz et al., 1987).

There also may be clinical significance to the observation that 2:1:0.5:0.5 skin ceramides:palmitic acid:cholesterol: cholesterol sulfate form the typical 130 Å repeating units, whereas 2:1:1 skin ceramides:palmitic acid:cholesterol sulfate produces a two-phase system. Thus, only a limited amount of cholesterol sulfate can be substituted for cholesterol in the fundamental repeating unit in the stratum corneum. Cholesterol sulfate is a small component of normal stratum corneum (~3% of the total lipid), but is elevated in skin scales (over 12% of the total lipid) in recessive X-linked ichthyosis (Williams and Elias, 1987).

The diffraction results presented here provide mechanistic information on the water permeability barrier afforded by the extracellular lipid lamellae. First, the wide-angle diffraction indicates that at 20°C there is a tight, gel-like packing of the lipid hydrocarbon chains, despite the relatively large concentration of cholesterol. In fact, the wide-angle spacing at 4.1 Å is at a slightly smaller spacing than that observed for typical gel phase phospholipids (Tardieu et al., 1973; McIntosh, 1980). Such tight chain packing would limit water movement across the extracellular multilayers. Previous X-ray diffraction and calorimetry studies provide evidence that similar tight hydrocarbon chain packing is present at physiological temperature. That is, there is no change in the 130 Å period and its associated wide-angle

pattern from 20°C to ~70°C in both intact stratum corneum (Bouwstra et al., 1995) and a skin ceramide:cholesterol:palmitic acid system (Bouwstra et al., 1996), and differential scanning calorimetry indicates that the melting of the lipid chains in stratum corneum occurs near 70°C (Van Duzee, 1975; Golden et al., 1986, 1987; Wertz and Downing, 1991). Secondly, there are extremely narrow fluid spaces between adjacent bilayers at low pH (similar to the environment in the stratum corneum) that would limit diffusion along the plane of the bilayers as found in phospholipid bilayers (Volke et al., 1994). Thus, the 130 Å structure described here would have relatively small water diffusion rates in directions both perpendicular and parallel to the plane of the bilayers.

REFERENCES

Abraham, W., and D. T. Downing. 1992. Lamellar structures formed by stratum corneum lipids in vitro: a deuterium nuclear magnetic resonance (NMR) study. *Pharm. Res.* 9:1415–1421.

Blaurock, A. E. 1971. Structure of the nerve myelin membrane: proof of the low-resolution profile. *J. Mol. Biol.* 56:35–52.

Bouwstra, J. A., F. E. Dubbelaar, G. S. Gooris, A. M. Weerheim, and M. Ponec. 1999. The role of ceramide composition in the lipid organization of the skin barrier. *Biochim. Biophys. Acta.* 1419:127–136.

Bouwstra, J. A., G. S. Gooris, W. Bras, and D. T. Downing. 1995. Lipid organization in pig stratum corneum. *J. Lipid Res.* 36:685–695.

Bouwstra, J. A., G. S. Gooris, K. Cheng, A. Weerheim, W. Bras, and M. Ponec. 1996. Phase behavior of isolated skin lipids. *J. Lipid Res.* 37:999–1011.

Bouwstra, J. A., G. S. Gooris, F. E. Dubbelaar, and M. Ponec. 2001. Phase behavior of lipid mixtures based on human ceramides: coexistence of crystalline and liquid phases. *J. Lipid Res.* 42:1759–1770.

Bouwstra, J. A., G. S. Gooris, F. E. Dubbelaar, and M. Ponec. 2002. Phase behavior of stratum corneum lipid mixtures based on human ceramides: the role of natural and synthetic ceramide 1. *J. Invest. Dermatol.* 118: 606–617.

Bouwstra, J. A., G. S. Gooris, J. A. Van Der Spek, and W. Bras. 1991. Structural investigations of human stratum corneum by small-angle x-ray scattering. *J. Invest. Dermatol.* 97:1005–1012.

Bouwstra, J. A., G. S. Gooris, J. A. Van Der Spek, S. Lavrijsen, and W. Bras. 1994. The lipid and protein structure of mouse stratum corneum: a wide and small angle diffraction study. *Biochim. Biophys. Acta.* 1212:183–192.

Brzustowicz, M. R., V. Cherezov, M. Caffrey, W. Stillwell, and S. R. Wassall. 2002. Molecular organization of cholesterol in polyunsaturated membranes: microdomain formation. *Biophys. J.* 82:285–298.

Costello, M. J., and T. Gulik-Krzywicki. 1976. Correlated x-ray diffraction and freeze-fracture studies on membrane model systems. *Biochim. Biophys. Acta.* 455:412–432.

Critchley, P. 1993. Skin lipids. *In* Molecular Aspects of Dermatology. G. C. Priestley, editor. John Wiley and Sons, Chichester, England. pp.147–169.

Downing, D. T. 1992. Lipid and protein structures in the permeability barrier of mammalian epidermis. *J. Lipid Res.* 33:301–313.

Elias, P. M., and D. S. Friend. 1975. The permeability barrier in mammalian epidermis. *J. Cell Biol.* 65:180–191.

Elias, P. M., J. Goerke, and D. S. Friend. 1977a. Mammalian epidermal barrier layer lipids: composition and influence on structure. *J. Invest. Dermatol.* 69:535–546.

Elias, P. M., N. S. McNutt, and D. S. Friend. 1977b. Membrane alterations during cornification of mammalian squamous epithelia: a freeze-fracture, tracer, and thin-section study. *Anat. Rec.* 189:577–594.

Forslind, B. 1994. A domain model of the skin barrier. *Acta Derm. Venereol.* 74:1–6.

Franks, N. P. 1976. Structural analysis of hydrated egg lecithin and cholesterol bilayers I. X-ray diffraction. *J. Mol. Biol.* 100:345–358.

Garson, J.-C., J. Doucet, J.-L. Leveque, and G. Tsoucaris. 1991. Oriented structure in human stratum corneum revealed by x-ray diffraction. *J. Invest. Dermatol.* 96:43–49.

Golden, G. M., D. B. Guzek, R. R. Harris, J. E. McKie, and R. O. Potts. 1986. Lipid thermotropic transitions in human stratum corneum. *J. Invest. Dermatol.* 86:255–259.

Golden, G. M., D. B. Guzek, A. H. Kennedy, J. E. McKie, and R. O. Potts. 1987. Stratum corneum lipid phase transitions and water barrier properties. *Biochemistry.* 26:2382–2388.

Hedberg, C. L., P. W. Wertz, and D. T. Downing. 1988. The nonpolar lipids of pig epidermis. *J. Invest. Dermatol.* 90:225–229.

Hou, S. Y., A. K. Mitra, S. H. White, G. K. Menon, R. Ghadially, and P. M. Elias. 1991. Membrane structures in normal and essential fatty acid-deficient stratum corneum: characterization by ruthenium tetroxide staining and x-ray diffraction. *J. Invest. Dermatol.* 96:215–223.

Inouye, H., and D. A. Kirschner. 1988. Membrane interactions in nerve myelin. I. Determination of surface charge from effects of pH and ionic strength on period. *Biophys. J.* 53:235–246.

Levine, Y. K., and M. H. F. Wilkins. 1971. Structure of oriented lipid bilayers. *Nat. New Biol.* 230:69–72.

Madison, K. C., D. C. Swartzendruber, P. W. Wertz, and D. T. Downing. 1987. Presence of intact intercellular lipid lamellae in the upper layers of the stratum corneum. *J. Invest. Dermatol.* 88:714–718.

McIntosh, T. J. 1980. Differences in hydrocarbon chain tilt between hydrated phosphatidylethanolamine and phosphatidylcholine bilayers. A molecular packing model. *Biophys. J.* 29:237–245.

McIntosh, T. J., and P. W. Holloway. 1987. Determination of the depth of bromine atoms in bilayers formed from bromolipid probes. *Biochemistry.* 26:1783–1788.

McIntosh, T. J., and S. A. Simon. 1986a. Area per molecule and distribution of water in fully hydrated dilauroylphosphatidylethanolamine bilayers. *Biochemistry.* 25:4948–4952.

McIntosh, T. J., and S. A. Simon. 1986b. The hydration force and bilayer deformation: a reevaluation. *Biochemistry.* 25:4058–4066.

McIntosh, T. J., S. A. Simon, J. C. Ellington, and N. A. Porter. 1984. A new structural model for mixed-chain phosphatidylcholine bilayers. *Biochemistry.* 23:4038–4044.

McIntosh, T. J., S. A. Simon, D. Needham, and C.-H. Huang. 1992a. Interbilayer interactions between sphingomyelin and sphingomyelin:cholesterol bilayers. *Biochemistry.* 31:2020–2024.

McIntosh, T. J., S. A. Simon, D. Needham, and C.-H. Huang. 1992b. Structure and cohesive properties of sphingomyelin:cholesterol bilayers. *Biochemistry.* 31:2012–2020.

McIntosh, T. J., M. E. Stewart, and D. T. Downing. 1996. X-ray diffraction analysis of isolated skin lipids: reconstitution of intercellular lipid domains. *Biochemistry.* 35:3649–3653.

McIntosh, T. J., and C. R. Worthington. 1974. Direct determination of the lamellar structure of peripheral nerve myelin at low resolution (17 Å). *Biophys. J.* 14:363–386.

Needham, D., and R. S. Nunn. 1990. Elastic deformation and failure of lipid bilayer membranes containing cholesterol. *Biophys. J.* 58:997–1009.

Scheuplein, R. J., and I. H. Blank. 1971. Permeability of the skin. *Physiol. Rev.* 51:702–747.

Shannon, C. E. 1949. Communication in the presence of noise. *Proc. Inst. Radio Engrs. NY.* 37:10–21.

Smaby, J. M., M. M. Momsen, H. L. Brockman, and R. E. Brown. 1997. Phosphatidylcholine acyl unsaturation modulates the decrease in interfacial elasticity induced by cholesterol. *Biophys. J.* 73:1492–1505.

Swartzendruber, D. C., P. W. Wertz, D. J. Kitko, K. C. Madison, and D. T. Downing. 1989. Molecular models of the intercellular lipid lamellae in mammalian stratum corneum. *J. Invest. Dermatol.* 92:251–257.

Tardieu, A., V. Luzzati, and F. C. Reman. 1973. Structure and polymorphism of the hydrocarbon chains of lipids: a study of lecithin-water phases. *J. Mol. Biol.* 75:711–733.

Torbet, J., and M. H. F. Wilkins. 1976. x-ray diffraction studies of lecithin bilayers. *J. Mol. Biol.* 62:447–458.

Van Duzee, B. F. 1975. Thermal analysis of human stratum corneum. *J. Invest. Dermatol.* 65:404–408.

Volke, F., S. Eisenblatter, J. Galle, and G. Klose. 1994. Dynamic properties of water at phosphatidylcholine lipid bilayer surfaces as seen by deuterium and pulsed field gradient proton NMR. *Chem. Phys. Lipids.* 70:121–131.

Wertz, P. W., and D. T. Downing. 1991. Epidermal lipids. *In* Physiology, Biochemistry, and Molecular Biology of the Skin. L. A. Goldsmith, editor. Oxford University Press, New York. pp.205–236.

Wertz, P. W., D. C. Swartzendruber, K. C. Madison, and D. T. Downing. 1987. Composition and morphology of epidermal cyst lipids. *J. Invest. Dermatol.* 89:419–425.

White, S. H., D. Mirejovsky, and G. I. King. 1988. Structure of lipid domains and corneocyte envelopes of murine stratum corneum. *Biochemistry.* 27:3725–3732.

Williams, M. L., and P. M. Elias. 1987. The extracellular matrix of stratum corneum: role of lipids in normal and pathological function. *CRC Crit. Rev. Therapeut. Drug Carr. Sys.* 3:95–122.

Worthington, C. R., G. I. King, and T. J. McIntosh. 1973. Direct structure determination of multilayered membrane-type systems which contain fluid layers. *Biophys. J.* 13:480–494.